Transition State Interactions in a Promiscuous Enzyme: Sulfate and Phosphate Monoester Hydrolysis by *Pseudomonas aeruginosa* Arylsulfatase

Bert van Loo[†1], Ryan Berry[‡], Usa Boonyuen[†,2], Mark F. Mohamed[†], Marko Golicnik[†,3], Alvan C. Hengge[*,‡] and Florian Hollfelder[*,†]

[†]Department of Biochemistry, University of Cambridge, Cambridge, United Kingdom

[‡]Department of Chemistry and Biochemistry, Utah State University, Logan, Utah 84322, United States

[1]Present address: Institute for Evolution and Biodiversity, University of Münster, Germany

[2]Present address: Faculty of Tropical Medicine, Mahidol University, Thailand

[3]Present address: Institute of Biochemistry, Faculty of Medicine, University of Ljubljana, Slovenia

*To whom correspondence should be addressed

ABSTRACT

Pseudomonas aeruginosa arylsulfatase (PAS) hydrolyses sulfate and, promiscuously, phosphate monoesters. Enzyme-catalyzed sulfate transfer is crucial to a wide variety of biological processes, but detailed studies of the mechanistic contributions to its catalysis are lacking. We present an investigation based on linear free energy relationships (LFERs) and kinetic isotope effects (KIEs) of PAS and active site mutants that suggest a key role for leaving group (LG) stabilization. In LFERs wild type PAS has a much less negative Brønsted coefficient ($\beta_{leaving\ group}^{obs\text{-}Enz}$ = -0.33) than the uncatalyzed reaction ($\beta_{leaving\ group}^{obs}$ = -1.81). This situation is diminished when cationic active site groups are exchanged for alanine. The considerable degree of bond breaking during the TS is evidenced by an $^{18}O_{bridge}$ KIE of 1.0088. LFER and KIE data for several active site mutants point to leaving group stabilization by active-site lysine K375, in cooperation with histidine H211. ^{15}N KIEs combined with an increased sensitivity to leaving group ability of the sulfatase activity in neat D_2O ($\Delta\beta_{leaving\ group}^{H\text{-}D}$ = +0.06) suggest that the mechanism for S-O_{bridge} bond fission shifts, with decreasing leaving group ability, from charge compensation via Lewis acid interactions towards direct proton donation. $^{18}O_{nonbridge}$ KIEs indicate that the TS for PAS-catalyzed sulfate monoester hydrolysis has a significantly more associative character compared to the uncatalyzed reaction, while PAS-catalyzed phosphate monoester hydrolysis does not show this shift. This difference in enzyme-catalyzed TSs appears to be the major factor favoring specificity toward sulfate over phosphate in this promiscuous hydrolase, since other features are either too similar (uncatalyzed TS) or inherently favor phosphate (charge).

INTRODUCTION

Arylsulfatases catalyze the *in vivo* hydrolysis of sulfate monoesters, producing inorganic sulfate, typically removing it from a sugar or a steroid hormone. Sulfatases are highly proficient enzymes, with catalytic proficiencies ($(k_{cat}/K_M)/k_{uncat}$) well above 10^{13}-10^{17} M^{-1} for the model substrate 4-nitrophenyl sulfate **1d** (Scheme 1).[1-3] Despite their occurrence in eukaryotes and prokaryotes, relevance for a variety of key processes (e.g. development,[4-10] germination,[11] resistance against toxic defense molecules,[12,13] mucin desulfation,[14-16] or degradation of mucopolysaccharides[17,18]) and the occurrence of various diseases as a result of their malfunction (e.g. lysosomal disorders[17,19]), their mechanism has not been studied in the same detail as that of the related phosphatases.

The majority of sulfatases known to date are members of the alkaline phosphatase (AP) superfamily. The mechanism of transition state (TS) stabilization during enzyme-catalyzed substrate hydrolysis of one member of this superfamily, *Escherichia coli* alkaline phosphatase (*Ec*AP), has been subject of a large number of in-depth studies involving the experimental tools of linear free energy relationships (LFERs), kinetic isotope effects (KIEs), mutant studies, and structural analysis by X-ray crystallography.[20-36] In addition computational simulations have been employed to pin-point transition state interactions.[26,27,37-41]

Sulfatase members of the AP superfamily have been studied less extensively. Catalytically important residues have been shown to be conserved among the arylsulfatases[2,42-47] and mutant studies (e.g. of human arylsulfatase A,[48] choline sulfatase,[47] and the closely related phosphonate monoester hydrolase[49]) have suggested that many of these conserved residues are indeed involved in the catalytic pathway in the enzyme active site. LFERs and KIEs have been measured for a number of phosphatases,[20-23,35,50-58] but only one such study is available for sulfatases.[59]

In addition to the family relationship, members of the AP superfamily are also typically catalytically promiscuous,[60-62] i.e. they catalyze multiple, chemically distinct reactions with large rate accelerations.[63,64] Within the superfamily reciprocal relationships of crosswise catalytic promiscuity are observed, i.e. the promiscuous activity of one member is the native function of another, and *vice versa*.[63,64] Given the postulated role of promiscuity in evolution by gene duplication,[60,65] functional crossover defines such functional relationships as pathways for respecialization or repurposing in enzyme superfamilies.[66] As catalysis for the activity under selective pressure must be maintained at a relevant level during evolution, the question of how mechanistic features of these enzymes can be effective for catalysis of different reactions arises.

We have studied the reactions catalyzed by the promiscuous arylsulfatase from *Pseudomonas aeruginosa* (PAS) using LFERs and KIEs. PAS has a wide active site opening[42] and – in contrast to sulfatases with high specificity for a particular leaving group (such as a sugar moiety[67,68] or choline[47]) – accepts a range of aromatic substrates: so that the construction of LFERs based on series of aryl sulfates of different reactivity is possible with minimal interference from unique binding effects. PAS operates at high rates (k_{cat}/K_M 4.9×10^7 $s^{-1}M^{-1}$), even for the hydrolysis of the non-natural substrate 4-nitrophenyl sulfate **1d.**[1] In addition, PAS promiscuously catalyzes the hydrolyses of phosphate mono-,[1] and diesters[62] as well as phosphonates,[69] thus covering mechanistically distinct hydrolase reactions.[70] However, despite its catalytic promiscuity, PAS is a genuine sulfatase: it is typically expressed under sulfate starvation conditions, part of an operon coding for sulfate-processing enzymes, and thought to act as a sulfate scavenger.[71,72]

Based on the X-ray structure of PAS[42] (and those of the human arylsulfatases A[45,73] (hASA) and B[43] (hASB) combined with mutant data for hASA[48]) a double displacement catalytic pathway was proposed, in which a post-translationally modified cysteine,[74]

formylglycine fGly51, performs a nucleophilic attack on the sulfur center (Figure 1b). The covalent hemiacetal intermediate is broken down with assistance of H115 acting as a general base (step 2 in Figure 1b). Finally the aldehyde form of the fGly nucleophile is again hydrated, regenerating the enzyme for the next round of catalysis. Mutant data for several of the analogous active site residues in hASA show that a single mutation into an alanine of one of the residues likely to be involved in charge compensation during the TS results in lowered but still detectable levels of activity.[48] During the hydrolysis of sulfates, negative charge is expected to build up in the TS on the sulfuryl group and on the leaving group.[3,75] TS stabilization can be achieved by offsetting this charge build-up: using positively charged functionalities such as metal ions, or by using hydrogen bonding or electrostatic interaction with positively charged amino acid side chains. The latter possibly may involve proton transfer to the leaving group oxygen. The active site of PAS contains a number of residues that could neutralize charge build-up on oxygen atoms during the transition state, or affect the pK_a of the formylglycine (fGly51) nucleophile (Figure 1).

Here we provide a detailed quantitative examination of their influence on the nature of the TS in the arylsulfatase-catalyzed reaction. We use LFER and KIE data to compare the nature of the TS for the native PAS-catalyzed sulfate monoester hydrolysis with the uncatalyzed reaction, and show that , while both are dissociative, the TS of the enzyme-catalyzed reaction has a more associative character. The latter difference is absent for phosphate monoester hydrolysis. Pre-steady-state kinetic data provide information about the rate-limiting step in the overall kinetic mechanism. Finally, changes in LFERs and KIEs as a result of alanine scanning mutagenesis of PAS active site residues suggest that Lys375 serves as the general acid that minimizes leaving group charge change in the TS and provides leaving group stabilization.

RESULTS AND DISCUSSION

Steady state parameters. In order to obtain insight into the nature of the transition state (TS) of PAS-catalyzed sulfate monoester hydrolysis we used a series of substrates with varying leaving groups to measure linear free energy relationships (LFERs), similar to those constructed for several phosphoryl transfer enzymes.[21,22,31,32,55-58,70,76]

Purified PAS WT[1] was used to determine Michaelis-Menten parameters k_{cat}, K_M and k_{cat}/K_M for a series of phenyl sulfate monoesters (compounds **1a**-**1l**, Scheme 1) with varying leaving group abilities (represented by their pK_a values, which range from 5.2 to 10.35 (Table S1 and Figures S1 and S2, supporting information, SI)). The steady-state catalytic rate constant (k_{cat}) is independent of leaving group ability (Figure 2a, varying between 9-18 s^{-1}; Table S1, SI). Based on the kinetic scheme for enzyme-catalyzed substrate hydrolysis (Figure 1c), the relevant rate constant to probe for information on the nature of the TS should be a good proxy for k_2. If enzyme-catalyzed cleavage of the sulfate ester bond were fully rate-limiting, the steady state catalytic rate constant k_{cat} would be essentially equal to k_2 (equation S14, SI). If this is not the case, i.e. if $k_2 \geq k_3$, more complex terms arise (see equations S1-3, SI). Assuming that the substrate binding constants ($K_D = k_{-1}/k_1$) are similar for the complete series of sulfate monoesters (Scheme 1), k_{cat}/K_M reports on all steps from free enzyme and substrate to the first irreversible transition state. In this case the formation of the covalent intermediate between the formylglycine nucleophile and the respective sulfur center of the substrates that leads to leaving group departure is likely to be irreversible, as no significant inhibition by the phenolate product is observed. (See equations S1-S3 in the SI for details on the relation between the Michaelis-Menten parameters and the individual rate constants for the various enzymatic steps).

Attempts to determine pre-steady state kinetics. Direct determination of pre-steady state kinetic parameters such as k_2 using stopped-flow methods requires a detectable burst phase. When the PAS WT-catalyzed hydrolysis of sulfate monoester **1d** was monitored at millisecond time-scale using a stopped-flow setup, only linear time courses without a burst phase were observed. This scenario does not rule out the existence of a burst, since a large ratio k_2/k_3 would make the relevant burst phase undetectable. When the time axis was corrected for the dead time of the equipment (3 ms), extrapolation of the linear time courses did not converge to the same point at t = 0 (Figure S3a, SI). The values for the positive intercepts at the product axis were directly correlated with the amount of active enzyme that was added (Figure S3b, SI), indicating the existence of a burst phase lasting less than 3 ms. This observation confirms an overall rate-limiting step that occurs after sulfate ester bond cleavage. Simulations of the stopped-flow time courses based on values for K_D, k_2 and k_3 that fit the steady state data (equations S5-7, Figure S4, SI) suggested that the actual K_D for substrate binding of sulfate monoester **1d** is at least 100 μM (i.e. >150-fold higher than its K_M). Simulation of the LFERs for k_{cat} and $1/K_M$ based on the same three pre-steady state parameters confirmed this observation (assuming K_D is equal for all substrates, Figure S5, SI). Consistent with k_3 being rate-limiting for the entire LFER, the apparent K_M values for the substrate series increased with increasing leaving group pK_a (from 0.6-28 μM, Table S1, SI) and log plots of k_{cat}/K_M and $1/K_M$ versus leaving group pK_a showed similar slopes of -0.33±0.04 and -0.31±0.04 respectively (Figure 2a). Since k_{cat} is more or less equal to k_3, which is independent of intrinsic substrate reactivity, it cannot be used as a proxy for the rate relevant to the LFER. We therefore use k_{cat}/K_M as a proxy for k_2.

LFER for PAS WT-catalyzed sulfate monoester hydrolysis. Plots of k_{cat}/K_M against the leaving group pK_a (Figure 2) were linear, with a $\beta_{leaving\ group}^{obs}$ of -0.33 that was considerably

less negative than that of the rate for the uncatalyzed hydrolysis reaction (k_{uncat}), for which a $\beta_{leaving\ group}^{obs}$ of -1.81 has been measured.[3] Williams *et al.*[59] recently constructed a LFER for PAS, but arrived at a much steeper slope (-0.86). Although most points superimpose well with our data (see Figure S6, SI), the choice of bulky leaving groups with higher pK_a (specifically the inclusion of the bulky 4-amino-acetyl- and 4-methoxyphenolate), the narrower range of pK_a-values (three compared to almost five log units covered here) as well as basing the study on overall fewer data points (7 *vs* 12 in our work) with worse significance (p-value, 0.026 *vs*. $<10^{-4}$) and correlation coefficients (R^2, 0.66 *vs*. 0.91) seem to have resulted in a distortion of the slope due to idiosyncratic effects of substrates (e.g. due to steric clashes). However, in both cases the slope $\beta_{leaving\ group}^{obs}$ is less steep than that for the solution reaction.

A possible cause for the considerably less negative $\beta_{leaving\ group}^{obs}$ compared to the solution reaction could be that the k_{cat}/K_M-values do not only represent a chemical step, as shown previously for wild-type *E. coli* alkaline phosphatase (AP).[34,52,77] Fast enzymatic reactions (k_{cat}/K_M ~10^6-10^9 s^{-1} M^{-1}) can be diffusion controlled, i. e. a physical step that occurs prior to the first chemical step can be rate-limiting. The k_{cat}/K_M-values for the PAS WT-catalyzed hydrolysis of sulfate monoesters **1a**-**1l** ranged from 10^5-10^7 s^{-1} M^{-1} (Table S1), which partially fall in the range mentioned above. In terms of the physical and chemical steps that occur during the reaction cycle of PAS (Figure 1c), diffusion control of k_{cat}/K_M arises when k_1×[S] is smaller than k_2 (which means $k_{-1} << k_2$). In extreme cases k_{cat}, K_M and k_{cat}/K_M can even be completely independent of k_2 (equations S11-13, SI). Since k_2 is expected to decrease with increasing pK_a, this extreme scenario is most likely for substrates bearing leaving groups with low pK_a, resulting in a flattening of the LFER. In this case the resulting $\beta_{leaving\ group}^{obs}$ will be less steep than the actual $\beta_{leaving\ group}$ of the chemical reaction of interest (step 2 in Figure 1b). Diffusion controlled reactions are known to be slowed down when

performed in increasingly viscous conditions. Viscosity dependence data for the PAS WT-catalyzed conversion of sulfate monoesters **1c** and **1d** showed a decrease in k_{cat}/K_M with increasing sucrose concentration (Figure S7). The decrease was the result of a decrease in k_{cat}, whereas K_M was unchanged. However, based on equations S1-3 (SI) K_M is expected to increase, whereas k_{cat} is expected to be unaffected by changes in the rate of substrate binding (k_1×[S]) or dissociation of the enzyme-substrate (ES) complex (k_{-1}), which are the steps expected to be affected by increased viscosity. Slowing down the dissociation of the final sulfate product would lower k_3 and thereby k_{cat}. However, K_M would decrease in this scenario as well (according to equation S9) and k_{cat}/K_M, which is independent from k_3, would be unchanged: yet this is not observed (Figure S7). At the high sucrose concentration used here it is not unlikely that even a weak molecular binding event causes inhibition. The data could be fitted to an inhibition constant of ~1.1 M for both k_{cat} and k_{cat}/K_M for both substrates. This suggests pure non-competitive inhibition of PAS by sucrose (20% (w/v) = 0.58 M), which would explain the observed lowering of k_{cat} and k_{cat}/K_M while K_M is unaffected (see the legend to Figure S7, SI, for more details). To test whether the LFER for PAS WT-catalyzed sulfate monoester hydrolysis was affected, data were recorded in 10% (w/v) sucrose and showed a $\beta_{leaving\ group}^{obs}$ identical to the one performed in the absence of the viscogen (Figure S8). Since the viscosity dependence is strongest for faster reactions, a diffusion-controlled reaction is expected to show a *less* negative $\beta_{leaving\ group}^{obs}$ in media with increased viscosity. We therefore conclude that the observed kinetic parameters that is relevant for monitoring leaving group effects for PAS WT-catalyzed hydrolysis of sulfate monoesters **1a**-**1l** are not diffusion controlled and that the deviation of $\beta_{leaving\ group}^{obs}$ from the $\beta_{leaving\ group}$ of the solution reaction is a genuine effect of substrate binding and turnover by the enzyme.

Previous experimental studies into the nature of the TS of enzyme-catalyzed sulfate transfer using LFERs[59,78] typically show less steep correlations than the corresponding

solution reaction,[79-82] bringing the Brønsted slopes to values closer to zero. This decrease could be ascribed to interactions with cationic groups in the active site, but no KIEs or mutational data were available to check this hypothesis. In addition a LFER for sulfate transfer has been reported for the promiscuous sulfatase activity of AP WT.[30] Subsequent KIE studies showed that in this case a dissociative TS is likely.[20] In AP the less negative $\beta_{leaving\ group}^{obs}$ compared to the solution reaction was explained by interaction of the leaving group with positively charged moieties in the enzyme active site, most likely a divalent metal ion (Zn^{2+}). The latter phenomenon has also been reported for AP-catalyzed phosphate monoester hydrolysis.[83] In several protein tyrosine phosphatases a protonated aspartate was identified as responsible for leaving group stabilization.[50,51,53-55,58] Replacement of this aspartate with asparagine restored the leaving group dependence to a value close to that of the solution reaction.[55] In protein phosphatase 1 (PP1), a histidine was thought to provide the same role, although practical limitations (low yield and poor activity) prevented experimental verification.[57]

LFER for PAS WT-catalyzed phosphate monoester hydrolysis. The fact that PAS WT is also a proficient phosphatase[1] ($(k_{cat}/K_M)/k_{uncat} = 2.9\times10^{11}$ M^{-1} towards phosphate monoester **2d**), opens up the possibility to study two reactions that proceed through similar TSs in solution[30,52,75,84-86] in a single active site, and also facilitates comparisons with the more widely studied phosphatases.

Michaelis-Menten parameters were determined for a series of phosphate monoesters (**2b-2l,** Scheme 1). As for the sulfatase reaction, k_{cat} is practically independent of the leaving group pK_a (varying between 0.6-1.2×10^{-2} s^{-1}, Figure 2i and Table S3, SI), suggesting that the rate-limiting step for phosphate as well as sulfate monoesters is not leaving group-dependent. The K_M values increase with leaving group pK_a and range from 0.03-0.92 mM,

around ~100-fold higher than for sulfatase activity. The slope of the Brønsted plot $\beta_{leaving\ group}^{obs}$ for k_{cat}/K_M for phosphate monoester hydrolysis is -0.39±0.04, identical within the error margins to the value observed for the sulfatase reaction (and confirmed by a cross-correlation graph with a slope of unity, see Figure S9, SI). As observed for the sulfatase reaction, enzyme-catalyzed phosphate monoester hydrolysis is considerably less sensitive to leaving group ability than the solution reaction for the phosphate monoester dianion ($\beta_{leaving\ group}$ = -1.23[86]). As for sulfate monoester hydrolysis, these considerable deviations can be caused by stabilization/masking of locally developing negative charge, in particular on the leaving group oxygen. Kinetic isotope effect studies suggested that the TS is similar to the solution reaction (see below for details), as in previously studied phosphatases.[22,36,55,57,58]

The effect of mutations on the $\beta_{leaving\ group}^{obs}$ for sulfate monoester hydrolysis. As discussed above, the $\beta_{leaving\ group}^{obs}$ of enzyme-catalyzed phosphate and sulfate transfer reactions can be influenced by compensation by positively charged moieties in the active site of the negative charge build-up that occurs during the TS.[22,32,36,57,78] Furthermore the change in nucleophile between the solution (H_2O) and enzyme-catalyzed (formylglycine) reaction can also influence the $\beta_{leaving\ group}^{obs}$. Zalatan *et al.*[36] formulated these considerations in order to be able to calculate expected differences in leaving group dependence between enzyme-catalyzed ($\beta_{leaving\ group}^{Enz}$) and solution reactions ($\beta_{leaving\ group}^{solution}$) (equation 1). The expected change in leaving group dependence resulting from a change in nucleophile between the enzyme-catalyzed (fGly) and solution (H_2O) reaction is calculated from the difference in nucleophilicity (pK_{nuc}^{Enz} - $pK_{nuc}^{solution}$) weighed with the sensitivity of the leaving group dependence of the reaction type to a change in nucleophile (p_{xy}). The second of the contributing factors is leaving group dependent binding of the ground state (GS, β_{bind}^{GS}) and

TS (β_{bind}^{TS}). For k_{cat}/K_M-based $\beta_{leaving\ group}$ values the latter two are indistinguishable from each other and are treated as a single variable ($\sum\beta_{bind} = \beta_{bind}^{GS} + \beta_{bind}^{TS}$).

$$\beta_{leavinggroup}^{Enz} = \beta_{leavinggroup}^{solution} + p_{xy} \times \left(pK_{nuc}^{Enz} - pK_{nuc}^{solution} \right) + \beta_{bind}^{TS} + \beta_{bind}^{GS} \qquad \text{(eq. 1)}$$

For *E. coli* AP in particular the interaction of the leaving group oxygen with one of the two Zn^{2+} ions during the GS and TS was thought to be mainly responsible for the $\sum\beta_{bind}$ of +0.33[83] (3-times larger than the expected contribution of the change in nucleophile from H_2O to the active site serine of +0.11). Selective removal of only the Zn^{2+}-ion responsible for leaving group stabilization is not feasible and therefore experimental assessment of these calculations was not possible. The assignment of the analogous positions of the nonbridging and bridging (leaving group) oxygens in an inorganic sulfate molecule with the active site residues of PAS (as shown in the X-ray structure,[42] Figure 1), was based on homology with structural data for the enzyme-substrate complex of an inactive variant of human arylsulfatase A.[73] The majority of the interactions with the nonbridging and leaving group oxygens are expected to be provided by amino acid side-chains, which opens up the possibility of assessing the importance of the correction factors of equation 1 experimentally by determining the leaving group dependence of active site mutants of PAS. To this end the nucleophile (fGly51) and a residue that directly interacts with it (H115) were mutated to assess the contribution of the nucleophile. Furthermore, several positively charged groups expected to provide charge compensation during the GS and TS by interacting with non-bridging (K113 and K375) and leaving group (H211 and K375) oxygens were removed by mutating the respective residues into alanine or leucine.

All mutants were purified to homogeneity and Michaelis-Menten parameters determined for the same series of sulfate monoesters (**1a**-**1l**, Scheme 1) as used with the

wild-type enzyme. The mutations resulted in 10^3-10^8-fold drops in catalytic efficiencies (k_{cat}/K_M) for the various substrates (Tables S4-S8, SI). For mutants C51S and H211A k_{cat} was still independent of leaving group ability (Figure 2b and 2e respectively), suggesting that, as in the wild-type enzyme, the leaving group-dependent step is not rate limiting. However the k_{cat} for these mutants was reduced ~10^3-fold (C51S) and ~10^5-fold (H211A) compared to PAS WT. The K_M values for PAS C51S and H211A were within an order of magnitude of those for the wild-type enzyme (Tables S4 and S7) and, as observed for wild-type PAS, the $\beta_{leaving\ group}^{obs}$ values for k_{cat}/K_M and $1/K_M$ are nearly identical. For PAS K113L and H115A both k_{cat} and $1/K_M$ decreased with increasing leaving group ability (Figure 2c and d, Table S5 and S6), albeit it only at the higher end of the pK_a spectrum for H115A. For PAS K375A k_{cat} decreases with increasing leaving group pK_a, indicating that the rate-limiting step is largely leaving group dependent. The K_M-values are increased ~10^3-fold compared to the wild-type enzyme and are largely constant (varying in a range of 5-10 mM) for the substrates with a leaving group pK_a > 8 (Figure 2f, Table S8). The $\beta_{leaving\ group}^{obs}$ for k_{cat}/K_M is nearly identical to that for k_{cat} for pK_a > 8. As for PAS WT, the LFERs for k_{cat} and $1/K_M$ for PAS K113L, H115A and K375A could be simulated based on assumed values for the pre-steady state kinetic parameters (Figure S10, SI). In particular for K113L and K375A the break in the LFER for k_{cat} could be explained by a change of the rate-limiting step with increasing $pK_a^{leaving\ group}$.

The $\beta_{leaving\ group}^{obs}$ of all active-site mutants was less negative than the $\beta_{leaving\ group}^{obs}$ for the wild type. $\Delta\beta_{leaving\ group}$ ($=\beta_{leaving\ group}^{obs\text{-}WT} - \beta_{leaving\ group}^{obs\text{-}mutant}$) was calculated as the slope of the linear correlation of $\log[(k_{cat}/K_M)_{WT}/(k_{cat}/K_M)_{mutant}]$ *vs*. $pK_a^{leaving\ group}$ (Table 2, Figure S11a). As described above the difference in leaving group dependencies between enzyme-catalyzed and uncatalyzed sulfate and phosphate monoester hydrolysis is influenced by the nature of the nucleophile and charge compensation effects (equation 1). Based on the pH-rate profile

for PAS-catalyzed sulfate monoester hydrolysis the pK_{nuc} of the enzyme is expected to be < 7.2[1]. The p_{xy}-value for sulfate transfer is not known, but is expected to be similar to the value for phosphate monoesters (0.013[87]). Assuming that the pK_{nuc}^{Enz} ~ 6 and $pK_{nuc}^{solution}$ = -1.7 (nucleophile = H_2O), the effect of the change in nucleophile between the PAS WT-catalyzed and the solution reaction is expected to be 0.013×(6-(-1.7)) = +0.10. Assuming the difference in nucleophilicity between fGly (solution pK_a ~ 13-14[88]) and serine (pK_a ~ 16, similar to that of ethanol) in solution translates into the same difference in the enzyme active site, a small increase in the contribution of the nucleophile term in equation 1 is expected for mutant C51S. Based on this assumption the $\Delta\beta_{leaving\ group}^{WT-C51S}$ is expected to be small and negative. However, we measure a value of +0.10 (Table 2). Since fGly is interacting directly with the Ca^{2+}-ion, changing it to a serine may cause a change in the charge compensation effects provided by the divalent cation, which could explain the positive value for $\Delta\beta_{leaving\ group}^{WT-C51S}$. Removal of H115 is expected to result in a slight increase in the pK_a of the nucleophile, again predicting a small negative $\Delta\beta_{leaving\ group}^{WT-H115A}$ as a result. However, the measured value of +0.32 suggests that any small effect of the mutation on the nucleophile term is overshadowed by a considerable decrease in $\sum\beta_{bind}$.

The removal of the residues that directly interact with the leaving group oxygen is expected to have a large effect on $\sum\beta_{bind}$, whereas groups that interact only with the non-bridging oxygens are expected to contribute to $\sum\beta_{bind}$ at ~10% of the value expected for direct interactions with the leaving group oxygen.[36] Mutation of H211 resulted in a $\Delta\beta_{leaving\ group}^{WT-H211A}$ of only +0.16, even though this residue interacts exclusively with be the leaving group oxygen. Removal of the nearby K375 results in a $\Delta\beta_{leaving\ group}^{WT-K375A}$ of +0.61. Since the removal of a positive charge is expected to increase the pK_{nuc}^{Enz}, the actual effects on $\sum\beta_{bind}$ may be slightly higher than observed. These data suggest that K375 is largely responsible for leaving group stabilization. However, unlike in PTPase[55], where a protonated

aspartate has been ascribed to performing the same function, its removal does not result in a near-complete abolition of the difference between $\beta_{leaving\ group}^{obs\text{-}Enz}$ and $\beta_{leaving\ group}^{obs\text{-}solution}$, since $\Delta\beta_{leaving\ group}^{PAS\ K375A\text{-}solution} = +0.87$. Values of ~+0.1-0.2 would be expected in case of complete removal of charge compensation on the leaving group as a result of the mutation (i.e. $\sum\beta_{bind} = 0$, only the change in nucleophile results in a small positive $\Delta\beta_{leaving\ group}^{obs}$). This observation could be rationalized by partial compensation of the loss of charge offset provided by K375 by nearby H211. The same phenomenon (i.e. that K375 partially assumes the role of H211) could explain the relatively small effect of mutation H211A on $\beta_{leaving\ group}^{obs}$. The combined effects of these two residues find support in the double mutant enzyme PAS H211A/K375A, for which no sulfatase activity was detectable ($k_{cat}/K_M < 5\times10^{-6}$ s^{-1} M^{-1} for sulfate monoester **1d**, see SI for consideration of the experimental detection limit). This observation strengthens the idea that the effect of each mutation is buffered by the nearby presence of a residue that can take over its function: if the measured reductions in activity for the single mutants were simply additive, the expected k_{cat}/K_M for sulfate monoester **1d** should be 2.6×10^{-3} s^{-1} M^{-1} (according to equation S21, SI), and still be detectable. By contrast, their cooperativity leads to a larger detrimental effect, when both are removed.

As discussed above the effect of leaving group dependent ground and transition-state binding ($\sum\beta_{bind}$) is expected to be modest for residues that interact mainly with the non-bridging oxygens: ~10% (for all the non-bridging oxygens combined) of the value expected for leaving group oxygen[83]. This consideration suggests that the maximal combined effect of K113, K375 and Ca^{2+} on $\sum\beta_{bind}$ *via* interactions with the non-bridging oxygens is expected to be ~+0.13 ($10/110\times(\beta_{leaving\ group}^{obs\text{-}WT} - \beta_{leaving\ group}^{obs\text{-}solution}) = 0.09\times(-0.33-(-1.81))=+0.13$). Since removal of a positive charge is expected to increase the pK_{nuc} of the enzymatic reaction, the observed effect on $\sum\beta_{bind}$ of the interaction with non-bridging oxygens, as a result of removing any of these three functional groups is expected to be <+0.05. However, mutation

K113L results in a $\Delta\beta_{leaving\ group}^{WT\text{-}K113L}$ of +0.24. This large effect partly explains why removal of H115 has an unexpectedly large $\Delta\beta_{leaving\ group}^{WT\text{-}H115A}$ of +0.32, since H115 and K113 interact closely in the 3D structure of PAS. The large effect of mutations C51S, K113L and H115A on PAS activity suggests that these mutations influence the interaction of the H211A/K375A pair with the leaving group oxygen. If the effects were electrostatic and isolated from the interactions with the leaving group oxygens, the effect of these mutations would be expected to be identical in K375A and WT, i.e. these three mutations should be additive to mutation K375A. The combined effects of K113L and K375A result in completely inactive enzyme ($k_{cat}/K_M < 5\times10^{-6}$ s^{-1} M^{-1} for sulfate monoester **1d**), which is lower than the expected value (7.0×10^{-4} s^{-1} M^{-1}; based on eq. S21, SI) for an additive effect of both mutations. This can be explained by interaction of both K113 and K375 with the non-bridging oxygens, in which case their simultaneous removal most likely results in complete abolition of substrate binding. The introduction of mutations C51S and H115A into the K375A variant does result in enzymes with detectable activities. However, the effect on the $\beta_{leaving\ group}^{obs}$ is much lower in the K375A mutant than in the wild-type enzyme, if present at all (C51S in K375A has no significant effect on $\beta_{leaving\ group}$, see Table 2 and Figure S10b for details). The non-additive behavior suggests that the unexpectedly large value of $\Delta\beta_{leaving\ group}^{WT\text{-}mutant}$ for both these mutations is due to their effect on the interactions between the leaving group oxygen and K375, i.e. this effect cannot be achieved unless K375 is present. Possible explanations for this phenomenon are (*i*) changes in the overall electrostatic character of the active site as result of the mutations that decrease the strength of the interaction between K375 and the leaving group oxygen or (*ii*) changes in substrate positioning that cause the optimal configuration of the K375-leaving group oxygen paring to be distorted, resulting in a lower contribution of this interaction to TS stabilization.

Kinetic Isotope Effects (KIEs). Kinetic isotope effects were measured for the bridging (or leaving group) and non-bridging oxygens as well as the nitro group for enzyme-catalyzed hydrolysis of sulfate monoester **1d** and phosphate monoester **2d** (Figure 3; Chart S1, SI), to complement the Brønsted analysis above [55,57]. The KIE experiment requires turnover of approximately half of a 100 μmol sample of labeled substrate. With mutants of low activity this can require long reaction times, or unpractically large amounts of enzyme. For that reason, most but not all of the mutants for which kinetic data are presented have accompanying KIE data in Table 3.

Because the KIEs were measured by the internal competition method they describe effects on k_{cat}/K_M (or V/K),[89] which, as described above, is representative of the rate constant for the first chemical step (k_2 in Figure 1c). Thus, the KIEs determined here reflect the TS for the substrate reacting with the formyl glycine nucleophile, even though the overall rate-determining step is breakdown of the intermediate.*

The expected ranges of the isotope effects in sulfate monoester **1d** and phosphate monoester **2d** and their interpretation have been discussed in detail previously.[90,91] The secondary KIE at the nitrogen atom, $^{15}(V/K)$, reports on negative charge development on the nitrophenolate leaving group in the transition state. The *p*-nitrophenolate anion has contributions from a quinonoid resonance form, with decreased N-O bond order and increased N-C bond order. Because N-O bonds are tighter in terms of vibrational frequencies, the nitrogen atom is more tightly bonded in neutral *p*-nitrophenol (or in the *p*NPP substrate) than in the phenolate anion. Thus, the ^{15}K EIE for deprotonation of *p*-nitrophenol is normal.(Original reference for this: Hengge, A. C.; Cleland, W. W. Direct measurement of transition-state bond cleavage in hydrolysis of phosphate esters of p-nitrophenol. *J. Am. Chem. Soc.* 1990, *112*, 7421-7422. When protonation or other interactions maintain the leaving group in a neutral state, there is no isotope effect (KIE =

unity). This KIE reaches its maximum value of about 1.003, reflecting a full negative charge, when the leaving group in the TS has a very high degree of bond fission and no interactions are neutralizing the resulting charge. The KIE at the bridge oxygen atom, $^{18}(V/K)_{bridge}$, is a primary isotope effect that arises from S-O or P-O bond fission and is also affected by O-H bond formation, if the leaving group is simultaneously protonated in the TS. Bond fission produces normal isotope effects, primarily due to reduction of the stretching vibration in the TS as the force constant is lowered. Protonation of this atom in the TS gives rise to inverse effects, from the new vibrational modes introduced from the forming bond. A large body of data from phosphate and sulfate ester hydrolysis shows the isotope effect from P-O or S-O bond fission is normally larger in magnitude than the inverse effect from protonation. A normal $^{18}(V/K)_{bridge}$ effect near its maximum of 1.03 reflects a largely broken S-O or P-O bond in the TS, arising from loss of vibrations involving this bond. In native enzymes utilizing general acid catalysis, or uncatalyzed reactions under acidic conditions, the observed $^{18}(V/K)_{bridge}$ is reduced by protonation, as shown in Table 3.

The leaving group KIEs $^{15}(V/K)$ and $^{18}(V/K)_{bridge}$ report on how leaving group stabilization might be compromised by mutation. Loss of general or Lewis acid catalysis will result in increases in both of these KIEs relative to the native enzyme. The isotope effect on the nonbridging oxygen atoms, $^{18}(V/K)_{nonbridge}$, monitors the hybridization state of the transferring sulfuryl or phosphoryl group, which affects the P-O or S-O nonbridging bond orders and hence their vibrational frequencies. A loose transition state gives rise to slightly inverse effects as these bond orders increase. This isotope effect becomes increasingly normal (i.e. approaching or exceeding a value of 1) as the transition state grows more associative in nature.

The small $^{15}(V/K)$ of 1.0006 (Table 3), for PAS WT-catalyzed hydrolysis of sulfate monoester **1d** suggests nearly complete neutralization of the negative charge developing on

the leaving group from S-O bond fission. Similar neutralization occurs by intramolecular pre-equilibrium proton transfer during the uncatalyzed hydrolysis of neutral sulfate monoesters under acidic conditions[92] ($^{15}(V/K)$ = 1.0004). The $^{18}(V/K)_{bridge}$ KIE for the PAS-catalyzed reaction is similar to that of the uncatalyzed hydrolysis of the neutral monoester[92] and the AP-catalyzed sulfate monoester hydrolysis[20] (Table 3, Figure 4a). In both cases significant masking of leaving group charge development occurs due to intramolecular proton transfer, or interaction with a Lewis acid, respectively. The magnitude of $^{18}(V/K)_{bridge}$ is consistent with significant S-O_{bridge} bond fission concomitant with leaving group stabilization, either by interaction with a positively charged group (Lewis acid) or protonation. A similar observation has been made for phosphate monoester hydrolysis catalyzed by AP,[20] protein phosphatase 1[57] (PP-1) and several protein-tyrosine phosphatases (PTPs)[50,51,53,54,93] (Figure 4a, Table S15).

In the PAS WT-catalyzed hydrolysis of phosphate monoester **2d**, the $^{15}(V/K)$ and $^{18}(V/K)_{bridge}$ KIEs also indicate near complete neutralization of the charge on the leaving group, and significant P-O_{bridge} bond fission (Table 3, Figure 4a). The $^{18}(V/K)_{nonbridge}$ KIE for PAS WT-catalyzed hydrolysis of phosphate monoester **2d** was more inverse than for the uncatalyzed solution reaction of the dianion (0.9912 *vs* 0.9994; Table 3, Figure 4b), and is similar to the value for its hydrolysis by the superfamily member AP R166S (0.9925).[35] In the case of AP the inverse shift in this KIE was attributed to interactions of the phosphoryl group with the metal ions and hydrogen bonding residues at the active site. In the PAS reaction similar interactions are possible (Figure 1). For the PAS WT-catalyzed hydrolysis of sulfate monoester **1d** the $^{18}(V/K)_{nonbridge}$ is normal (1.0064, or + 0.64%, Table 3 and Figure 4b), in contrast to the inverse $^{18}(V/K)_{nonbridge}$ for the uncatalyzed hydrolysis of the **1d** monoanion[92] (-0.49%). This value is closer to the $^{18}(V/K)_{nonbridge}$ for the hydrolysis of the neutral sulfate monoester[92] (+0.98%). However, in this case, the normal KIE arises from

deprotonation of the sulfuryl group (i.e. proton transfer from S-O-H to the leaving group). In previous investigations of the TS for enzymatic sulfate and phosphate transfer the drop in the normal $^{18}(V/K)_{bridge}$ was accompanied by a more inverse[20] or mostly unchanged $^{18}(V/K)_{nonbridge}$ KIE[50,51,53-55,57,93] (compared to the $^{18}(V/K)_{nonbridge}$ for uncatalyzed phosphate dianion hydrolysis, i.e. ≤0.9994), and suggests that the TS in these enzymatic reactions is still largely dissociative despite the less negative $\beta_{leaving\ group}{}^{obs}$ and drop in normal $^{18}(V/K)_{bridge}$ KIE compared to the uncatalyzed reaction, which arise from neutralization of the charge developing on the leaving group. The normal $^{18}(V/K)_{nonbridge}$ is unlikely to arise from the same origin as in the uncatalyzed hydrolysis of the neutral sulfate monoester, since protonation of the sulfuryl group oxygens will not occur, except under extremely acidic conditions. A more plausible explanation is that the PAS WT-catalyzed TS is more associative than the solution reaction of the monoanion. The latter scenario could also partly explain the unexpectedly large effect of the removal of residues that only interact indirectly with the non-bridging leaving group oxygen on $\beta_{leaving\ group}{}^{obs}$.

The PAS K375A mutation results in a reaction for which the $^{15}(V/K)$ and $^{18}(V/K)_{bridge}$ KIEs are largely identical to those of the uncatalyzed hydrolysis (Table 3, Figure 4b), suggesting this residue is largely responsible for leaving group neutralization in the TS. This is consistent with the effect of the mutation on the $\beta_{leaving\ group}{}^{obs}$, and similar to what has been observed for the removal of an aspartic acid that performs a similar role in PTPs.[51,53,54] The data suggest that this residue either protonates the leaving group directly, or, that its mutation results in a dislocation of H211 (Figure 1), interfering with its function in this role, implying synergy between these two residues, as discussed earlier. The $^{18}(V/K)_{nonbridge}$ for PAS K375A is identical to the uncatalyzed hydrolysis, which could be explained by the loss of coordination of K375 to the sulfuryl group.

The relatively modest effect of the C51S mutation on $^{15}(V/K)$ and $^{18}(V/K)_{bridge}$ compared to the wild type reaction is consistent with the modest effect of this mutation on $\beta_{leaving\ group}{}^{obs}$. As stated above, the TS of the PAS WT-catalyzed sulfate monoester hydrolysis has a more associative character than in the uncatalyzed reaction, i.e. the nature of the nucleophile is thought to be more important, based on the change to a normal $^{18}(V/K)_{nonbridge}$. However, the change in nucleophile from fGly to serine has a much smaller effect on $^{18}(V/K)_{nonbridge}$, than the removal of K375, which is thought to interact directly with the nonbridging oxygens (Figure 1).

The mutation of H115 to alanine has a large effect on the KIEs compared to WT, despite the absence of direct TS interaction between H115 and the substrate (Table 3, Figure 4). The $^{18}(V/K)_{bridge}$ is nearly as large as that observed for PAS K375A. The $^{15}(V/K)$ shows partial charge neutralization on the leaving group, intermediate between the WT reaction and that of K375A. A possible explanation is suboptimal orientation of the substrate relative to the residues mainly responsible for leaving group stabilization, K375 and H211. The reaction of the H115A mutant shows a $^{18}(V/K)_{nonbridge}$ that is also intermediate between the WT and K375A, also consistent with less than optimal coordination of the non-bridging oxygens to K375. The fact that mutation H115A has a larger effect on $^{18}(V/K)_{nonbridge}$ than C51S confirms that the large change in $^{18}(V/K)_{nonbridge}$ for the PAS WT-catalyzed reaction compared to the sulfate monoester monoanion uncatalyzed hydrolysis is most likely not dependent on the nucleophile, but the result of interactions between the nonbridging oxygens and positively charged functional groups (K113, K375 and Ca^{2+}). The nature of the contribution of the latter interactions to TS stabilization appears to be unique for PAS WT-catalyzed sulfate monoester hydrolysis, since the effect of the enzyme on the $^{18}(V/K)_{nonbridge}$ for phosphate monoester hydrolysis is completely different. However, both reactions show a similar degree of leaving group stabilization.

Leaving group dependence in D_2O. The considerably less negative $\beta_{leaving\ group}^{obs}$ and a ^{15}N KIE near unity for the PAS WT-catalyzed sulfate monoester hydrolysis could be caused by protonation of the leaving group oxygen, as in PTPs.[51,53-55,58] Lewis acid charge neutralization by metal ions can have the same effect.[20] The available data for PAS all point to K375 as the main residue responsible for stabilization of charge that develops on the leaving group oxygen in the TS. Direct proton transfer involving lysine as the donor in enzyme active sites is rare, and charge compensation by Lewis acid interaction with the cationic charge of the protein shared between H211 and K375 is a potential alternative. The PAS WT-catalyzed sulfate monoester hydrolysis in D_2O is more sensitive to the leaving group ($\beta_{leaving\ group}$ is more negative) compared to the same reaction in H_2O (Figure S12). The observed difference in leaving group dependence ($\Delta\beta_{leaving\ group}^{H\text{-}D}$) is +0.06±0.03, which corresponds to a k_H/k_D ratio ranging from ~1.7 at $pK_a^{leaving\ group} = 5.5$ to ~3.3 at $pK_a^{leaving\ group} = 10$. These data suggest that with increasing demand for leaving group stabilization, a proton transfer event becomes more rate-limiting. This would suggest that the degree of $S\text{-}O_{bridge}$ bond fission during the TS is reduced with increasing leaving group ability (i.e. $S\text{-}O_{bridge}$ bond fission is almost complete prior to proton transfer for the low pK_a leaving groups that require charge offset assistance less). However, the ^{15}N KIE for PAS WT-catalyzed hydrolysis of sulfate monoester **1d** (pK_a = 7.02) suggests almost complete charge compensation on the leaving group oxygen, suggesting K375 is mainly responsible for charge compensation without transferring its proton during catalysis. For PAS K375A, there is no difference in $\beta_{leaving\ group}^{obs}$ when recorded in H_2O or D_2O (Figure S13). However, a pK_a-independent k_H/k_D of ~2 for all reactions was observed, suggesting that a leaving group independent proton transfer event is rate-limiting for this mutant. The solvent isotope effect is consistent with the suggested catalytic role for K375 as the main residue responsible for

leaving group stabilization during bond-breaking in the TS, since any leaving group dependent proton transfer event will most likely be fast compared to the severely slowed down S-O_{bridge} bond fission. Indeed, the heavy-atom isotope effects suggest that these two events occur in the same step.

IMPLICATIONS AND CONCLUSIONS

A mechanistic pathway for PAS WT-catalyzed sulfate monoester hydrolysis (Figure 1b) had been suggested by structural analysis, but can now be firmly established on the basis of the results presented in this study, including a reassessment of the contributions of the active site residues. For example, leaving group stabilization by the proposed general acid H211 is much less important than that of K375 (based on the much smaller effect on $\beta_{leaving\ group}^{obs}$ upon alanine scanning). The combined effect of removing both these residues was larger than the sum of its effects in wild-type enzyme, suggesting a high degree of interdependence between these two residues with regard to leaving group stabilization, possibly by sharing a proton (Figure 5). The LFERs for k_{cat} and $1/K_M$ for PAS WT-catalyzed sulfate monoester hydrolysis and the pre-steady-state measurements with sulfate monoester **1d** suggest that the leaving group dependent sulfate ester bond fission (S-O_{bridge} fission; step 1 in Figure 1b) is much faster than the cleavage of the hemiacetal intermediate (step 2, Figure 1b).

The strongest effect on leaving group dependent catalysis was seen for the K375A mutants ($\Delta\beta_{leaving\ group}^{obs}$ = +0.61, Figure 2f, Table 2), further underlining that K375 is the most important residue for stabilization of the negative charge that develops on the leaving group oxygen during catalysis. This conclusion was also supported by the following observations: (*i*) The ^{15}N and $^{18}O_{bridge}$ KIEs for mutant K375A are essentially the same as for

the solution reaction. The wild-type showed almost complete charge compensation on the leaving group (^{15}N KIE essentially unity) and a lowered normal $^{18}O_{brigde}$ KIE (Table 3, Figure 4). *(ii)* For PAS K375A the leaving group dependent step becomes increasingly more rate-limiting with decreasing leaving group ability (Figures 2f, S10b), pointing to its involvement in leaving group stabilization. (*iii*) The unexpectedly large effects on $\beta_{leaving\ group}^{obs}$ for active site mutants C51S and H115A are dependent on the presence of K375 (Table 2), suggesting that the main function of the other active site residues is to position the substrate for optimal interaction with K375. (*iv*) Structural alignment of PAS[42] with AP[94] shows that K375 occupies a similar position as the divalent metal ion thought to provide leaving group stabilization in AP (Figure 5).

Compensation of charge development on the leaving group oxygen by an amino acid side chain may be expected to involve direct protonation of the leaving group oxygen. The cleavage of this S-O_{bridge} ester is dependent on, and occurs in concert with a near-complete neutralization of the charge on the leaving group for sulfate monoester **1d** ($pK_a^{leaving\ group}$ = 7.03), as evidenced by a ^{15}N KIE near unity (Table 3). This would suggest near-complete proton transfer during the TS, but transfer of the proton, would only occur once the S-O_{bridge} bond cleavage is well advanced, if at all (Figures 5a and b). Charge compensation at the leaving group oxygen is near completion for PAS WT-catalyzed hydrolysis of sulfate monoester **1d**. As the proton is shared between H211 and K375 (Figures 5a and b) it may be that actual proton donation from lysine does not take place and instead transfer to H211 results in the observed compensation. Comparison of the leaving group dependences in H_2O and D_2O showed an increasing k_H/k_D ratio for k_{cat}/K_M with decreasing leaving group ability (Figure S12, SI), suggesting that proton transfer is becoming increasingly more important for S-O_{bridge} ester bond fission. The absence of the leaving group dependent change in k_H/k_D for PAS K375A (Figure S13) further supports the importance of K375 for S-O_{bridge} bond

fission, since it is in agreement with S-O_{bridge} ester bond fission being fully rate-limiting for leaving group departure in this mutant. (This solvent isotope effect is relevant for the first chemical step, while the isotope effect on k_{cat} reflects the overall rate-determining step, i.e. breakdown of the intermediate).

The correlation of reaction rates and the measured values for $\beta_{leaving\ group}^{obs}$ (Figure 6) establishes a direct link between charge compensation and catalytic efficiency: the more the catalytic effect of the proton is removed (as indicated by larger effective charge changes at the leaving group oxygen), the more does the overall rate suffer. This effect is more pronounced for unreactive substrates that require interaction with the proton held by K375 and H211 to a greater extent (Figure S15).

An alternative mechanistic scenario in which additional steps prior to the first irreversible S-O_{bridge} ester bond fission are rate limiting for wild-type, but the chemical step becomes limiting in a mutant may be considered. Such an explanation has been advanced for FLAP endonuclease, where pH-rate profiles suggested rate-limiting physical steps after substrate binding resulted in a commitment to catalysis that suppressed the magnitude of $\beta_{leaving\ group}^{obs}$ and was reduced or eliminated by a mutation that slowed the chemistry step.[95] However, this scenario is inconsistent with the observed KIEs on PAS catalysis. A commitment factor would reduce all the observed KIEs in equal proportion.),[89] Thus, if making the chemical step more rate-limiting (reducing a commitment factor) were the cause of the larger Brønsted slope, the KIEs would increase in the same proportion. Instead, the K375A mutant reaction gives an ^{15}N KIE that is 4-fold higher than wild-type PAS; the bridge ^{18}O effect is 2.8-fold greater; and the non-bridge ^{18}O effect goes from normal to inverse. The substrates in FLAP and PAS also show significant differences: DNA substrates of FLAP may require unpairing or helical arch ordering, whereas for the small molecule substrates of PAS no analogous steps are conceivable. In addition the high K_M-values are

consistent with reversibility and a rapid equilibrium between bound and unbound states (contrasting with the nM binding in FLAP). The LFERs and KIEs for PAS use k_{cat}/K_M comparisons that reflect the first irreversible step of the reaction, which thus is unlikely to be associated with binding.

Although the exact residues and functional groups involved differ between several previously characterised phosphatases[20,22,23,32,35,50,51,53-55,57,58,93] and PAS, all these enzymes rely on leaving group stabilization by charge compensation, resulting in less negative $\beta_{leaving\ group}^{obs}$ values and lowered, but still normal $^{18}O_{bridge}$ KIEs. However, the KIEs for PAS are consistent with a more associative mechanism than previously reported phosphatases, because of the observed change of $^{18}O_{nonbrigde}$ KIE from inverse (-0.49%) to normal (+0.62%) compared to the solution reaction (Table 3, Figure 4b). In phosphatases the small inverse $^{18}O_{nonbridge}$ KIE was either more inverse[20] or virtually unchanged[50,51,53,54,57,93] (Figure 4b, Table S15). The possible change from a dissociative to a more associative TS does not apply to all PAS-catalyzed conversions, since the promiscuous enzyme-catalyzed hydrolysis of phosphate monoester **2d** showed a more inverse $^{18}O_{nonbridge}$. Enzymatic specificity towards sulfate over phosphate monoester cannot be primarily based on overall charge, demand for leaving group stabilization or nucleophile strength, since these either provide no discrimination or will favor the more highly charged phosphate monoesters. The difference in effect on the $^{18}O_{nonbridge}$ KIE suggest that the subtle differences in geometry between the S-$O_{nonbridge}$ and P-$O_{nonbridge}$ bonds are responsible for making PAS specific toward sulfate monoesters.

More generally, the methodology developed here extends the use of physical-organic approaches to enzyme catalysis further, establishing the measurement of effective charge change *via* Brønsted plots for mutants as a way assess the involvement of a particular residue in catalysis. The correlation of catalyst and substrate reactivity (Figure 6) provides a further measure of sensitivity of reactivity changes and should be a quantitative measure of

the efficiency of general acid catalysis catalysis. In the future it will be interesting to contrast slopes in such double reactivity plots (as in Figure 6b) for several enzyme systems and use its slopes to quantify the sensitivity of catalytic effects in different active site arrangements.

EXPERIMENTAL SECTION

Sulfate monoester compounds for linear free energy relationships (LFERs) and kinetic isotope effect studies. Sulfate monoester **1d** and phosphate monoesters **2d** and **2k** (Scheme 1) were purchased from Sigma. Sulfate esters were synthesized from the respective phenol and chlorosulfonic acid, phosphate monoesters from phosphoryl chloride and the respective phenol. Detailed procedures are given in the SI. The isotopically labeled forms of 4-nitrophenyl sulfate (**1d**)[92] and phosphate (**2d**)[52] for measurement of kinetic isotope effects were synthesized as described previously.

Construction of mutants. All mutants of PAS, except for mutant C51S, which was constructed previously,[1] were made by site-directed mutagenesis according to the QuikChange protocol (Agilent), using primers listed in Table S16 (SI) and the appropriate template plasmid.

Protein production and purification. Expression of recombinant protein from plasmid pME4322[96] and derived mutants was done in *E. coli* BL21 (DE3) growing in LB or 2YT-medium containing 30 mg mL^{-1} kanamycin. The cells were grown at 37 °C until an OD_{600} of around 0.6-0.8 was reached. The culture was cooled to 30 (WT) or 20 °C (Mutants), IPTG was added up to 0.75 mM and the culture was grown for 4 hours at 30 °C (WT) or overnight at 20 °C (Mutants).

Cells expressing PAS were harvested by centrifugation and resuspended in 50 mM Tris-HCl pH 8.0. One tablet of Complete® EDTA-Free protease inhibitor cocktail (Roche) per 12 g of wet cell pellet was added to the suspension and the cells were lysed either by

using an emulsiflex-C5 homogenizer (Avestin) or by sonication. Cell-free extract (CFE) was obtained by centrifugation of the crude cell lysate at 30,000×g for 90 min. The PAS variants were purified from CFE by subsequent anion exchange (Q-sepharose), hydrophobic interaction (Phenyl sepharose), and size exclusion (Superdex 200) chromatography. All steps were performed in 50 mM Tris-HCl pH 8.0 with the appropriate additive for each step. The anion exchange chromatography was performed as described before.[1] Protein containing fractions that eluted from the anion exchange column were pooled and the combined fractions were brought to 200 mM $(NH_4)_2SO_4$ by adding the appropriate volume of 50 mM Tris-HCl pH 8.0 + 2 M $(NH_4)_2SO_4$ and subsequently loaded onto a phenyl sepharose hydrophobic interaction column. The column was washed with 2 column volumes (CV) of 50 mM Tris-HCl pH 8.0 +200 mM $(NH_4)_2SO_4$. Protein was eluted from the column with a gradient of 200-0 mM $(NH_4)_2SO_4$ in 50 mM Tris-HCl over 5 CV followed by a further 5 CV with 50 mM Tris-HCl pH 8.0. Fractions containing active protein were pooled and concentrated into 50 mM Tris-HCl pH 8.0 to around 10-15 mg mL^{-1} protein. The concentrated protein was loaded onto a Superdex 200 prep grade gel filtration column. PAS eluted at the expected elution volume of monomeric PAS. Protein containing fractions were pooled and concentrated to 100-350 μM in 50 mM Tris-HCl and aliquoted in appropriate portions, flash frozen in liquid N_2 and stored at -20 °C. Protein concentrations were calculated based on the molar extinction coefficient at λ = 280 nm, ε_{280} = 102790 M^{-1} cm^{-1}, calculated from the amino acid sequences using ProtParam (http://expasy.org/tools/protparam.html).

Enzyme kinetics. All data for steady state enzyme kinetics were recorded at 25 °C in 100 mM Tris-HCl pH 8.0 supplemented with 500 mM NaCl or as indicated. Observed initial rates (V_{obs}) were determined by following an increase in absorbance at a fixed wavelength (ranging from 270 to 400 nm depending on the substrate) as a result of product

formation over time in microtiterplates (Spectramax Plus, Molecular Devices) or quartz cuvettes (Varian 100 Bio). Catalytic parameters k_{cat}, K_M and/or k_{cat}/K_M were obtained by fitting the dependency of V_{obs} on substrate concentration ([S]) at a fixed enzyme concentration ([Enz]) (equation 2).

$$V_{obs} = \frac{k_{cat} \times [Enz] \times [S]}{K_M + [S]} \qquad \text{eq. 2}$$

The dependency of the various kinetic parameters (k_{cat}, $1/K_M$ and k_{cat}/K_M, represented by K in equation 3) on leaving group ability (as represented by their pK_a's) was fitted to equation 3 to obtain the observed Brønsted constants for leaving group dependence ($\beta_{leaving\ group}^{obs}$).

$$\log[K] = \beta_{leavinggroup}^{obs} \times pK_a^{leavinggroup} + C \qquad \text{eq. 3}$$

Stopped-flow kinetics. Fast kinetics for PAS WT-catalyzed hydrolysis of sulfate monoester **1d** were recorded using a SX20 stopped-flow setup (Applied Photophysics). No unambiguous burst phase could be detected with PAS concentrations between in 1 and 8 μM and 1 mM sulfate monoester **1d**, with 100 mM Tris-HCl pH 8.0, containing 500 mM NaCl at 20 °C. Data are shown in Figure S3.

Kinetic isotope effects (KIEs). Natural abundance **1d** or **2d** was used for measurements of $^{15}(V/K)$. The ^{18}O KIEs $^{18}(V/K)_{bridge}$ and $^{18}(V/K)_{nonbridge}$ were measured by the remote label method, using the nitrogen atom in *p*-nitrophenol as a reporter for isotopic fractionation in labeled bridging or nonbridging oxygen positions.[90] The particular isotopic isomers used are shown in the SI. Isotope effect experiments used 100 μmoles of substrate, at 25 °C in 50 mM Tris buffer, pH 8.0. The substrate concentration was 19 mM and the

reactions were started by addition of wild-type or mutant enzyme, 1 μM for substrate **1d**, and 725 μM for substrate **1b**. After reactions reached completion levels between 40% and 60% they were stopped by titration to pH 3 with HCl. Protocols for isolation of *p*-nitrophenol, isotopic analysis, and calculation of the isotope effects were the same as previously described,[52,92] and are described in the SI.

ASSOCIATED CONTENT

Supporting information available. Synthetic procedures, mathematical descriptions for enzyme kinetics and expected detection limits, determination of kinetic isotope effects and data analysis. Michaelis-Menten plots for sulfate substrates hydrolyzed by PAS WT, tables of experimentally measured steady-state kinetic parameters, additional LFERs, stopped flow data and primers used for mutant construction.

ACKNOWLEDGMENTS

This research was funded by the Biological and Biotechnological Research Council (BBSRC) and the Engineering and Physical Sciences Research Council (EPSRC) and NIH grant GM 47292 to ACH. FH is an ERC Starting Investigator, UB received a studentship from the Royal Thai Government and MG was supported by a postdoctoral Marie-Curie fellowship from the EU. We thank Marko Hyvonen for his help in the preparation of structural figures.

REFERENCES

(1) Olguin, L. F.; Askew, S. E.; O'Donoghue, A. C.; Hollfelder, F. *J. Am. Chem. Soc.* **2008**, *130*, 16547.

(2) van Loo, B.; Bayer, C. D.; Fisher, G.; Jonas, S.; Valkov, E.; Mohammed, M. F.; Vorobieva, A.; Dutruel, C.; Hyvonen, M.; Hollfelder, F. *Manuscript in prep.* **2015**.

(3) Edwards, D. R.; Lohman, D. C.; Wolfenden, R. *J. Am. Chem. Soc.* **2012**, *134*, 525.

(4) Haag, E. S.; Raff, R. A. *Dev. Genes Evol.* **1998**, *208*, 188.

(5) Sasaki, H.; Yamada, K.; Akasaka, K.; Kawasaki, H.; Suzuki, K.; Saito, A.; Sato, M.; Shimada, H. *Eur. J. Biochem.* **1988**, *177*, 9.

(6) Yamada, K.; Akasaka, K.; Shimada, H. *Eur. J. Biochem.* **1989**, *186*, 405.

(7) Yang, Q.; Angerer, L. M.; Angerer, R. C. *Dev. Biol.* **1989**, *135*, 53.

(8) Lai, J.; Chien, J.; Staub, J.; Avula, R.; Greene, E. L.; Matthews, T. A.; Smith, D. I.; Kaufmann, S. H.; Roberts, L. R.; Shridhar, V. *J. Biol. Chem.* **2003**, *278*, 23107.

(9) Morimoto-Tomita, M.; Uchimura, K.; Werb, Z.; Hemmerich, S.; Rosen, S. D. *J. Biol. Chem.* **2002**, *277*, 49175.

(10) Obaya, A. J. *Gene* **2006**, *372*, 110.

(11) Scott, W. A.; Metzenberg, R. L. *J. Bacteriol.* **1970**, *104*, 1254.

(12) Ratzka, A.; Vogel, H.; Kliebenstein, D. J.; Mitchell-Olds, T.; Kroymann, J. *Proc. Natl. Acad. Sci. U. S. A.* **2002**, *99*, 11223.

(13) Wittstock, U.; Fischer, M.; Svendsen, I.; Halkier, B. A. *IUBMB Life* **2000**, *49*, 71.

(14) Govan, J. R.; Deretic, V. *Microbiol. Rev.* **1996**, *60*, 539.

(15) Jansen, H. J.; Hart, C. A.; Rhodes, J. M.; Saunders, J. R.; Smalley, J. W. *J. Med. Microbiol.* **1999**, *48*, 551.

(16) Piotrowski, J.; Slomiany, A.; Murty, V. L.; Fekete, Z.; Slomiany, B. L. *Biochem. Int.* **1991**, *24*, 749.

(17) Diez-Roux, G.; Ballabio, A. *Annu. Rev. Genomics Hum. Genet.* **2005**, *6*, 355.

(18) Ghosh, D. *Cell. Mol. Life Sci.* **2007**, *64*, 2013.

(19) von Figura, K.; Schmidt, B.; Selmer, T.; Dierks, T. *Bioessays* **1998**, *20*, 505.

(20) Catrina, I.; O'Brien, P. J.; Purcell, J.; Nikolic-Hughes, I.; Zalatan, J. G.; Hengge, A. C.; Herschlag, D. *J. Am. Chem. Soc.* **2007**, *129*, 5760.

(21) Hall, A. D.; Williams, A. *Biochemistry* **1986**, *25*, 4784.

(22) Hollfelder, F.; Herschlag, D. *Biochemistry* **1995**, *34*, 12255.

(23) Holtz, K. M.; Catrina, I. E.; Hengge, A. C.; Kantrowitz, E. R. *Biochemistry* **2000**, *39*, 9451.

(24) Holtz, K. M.; Kantrowitz, E. R. *FEBS Lett.* **1999**, *462*, 7.

(25) Holtz, K. M.; Stec, B.; Kantrowitz, E. R. *J. Biol. Chem.* **1999**, *274*, 8351.

(26) Hou, G.; Cui, Q. *J. Am. Chem. Soc.* **2012**, *134*, 229.

(27) Hou, G.; Cui, Q. *J. Am. Chem. Soc.* **2013**, *135*, 10457.

(28) Kim, E. E.; Wyckoff, H. W. *J. Mol. Biol.* **1991**, *218*, 449.

(29) Nikolic-Hughes, I.; O'Brien P, J.; Herschlag, D. *J. Am. Chem. Soc.* **2005**, *127*, 9314.

(30) Nikolic-Hughes, I.; Rees, D. C.; Herschlag, D. *J. Am. Chem. Soc.* **2004**, *126*, 11814.

(31) O'Brien, P. J.; Herschlag, D. *J. Am. Chem. Soc* **1999**, *121*, 11022.

(32) O'Brien, P. J.; Herschlag, D. *Biochemistry* **2002**, *41*, 3207.

(33) O'Brien, P. J.; Lassila, J. K.; Fenn, T. D.; Zalatan, J. G.; Herschlag, D. *Biochemistry* **2008**, *47*, 7663.

(34) Simopoulos, T. T.; Jencks, W. P. *Biochemistry* **1994**, *33*, 10375.

(35) Zalatan, J. G.; Catrina, I.; Mitchell, R.; Grzyska, P. K.; O'Brien P, J.; Herschlag, D.; Hengge, A. C. *J. Am. Chem. Soc.* **2007**, *129*, 9789.

(36) Zalatan, J. G.; Herschlag, D. *J. Am. Chem. Soc.* **2006**, *128*, 1293.

(37) Luo, J.; van Loo, B.; Kamerlin, S. C. *FEBS Lett.* **2012**, *586*, 1622.

(38) Luo, J.; van Loo, B.; Kamerlin, S. C. *Proteins* **2012**, *80*, 1211.

(39) Lopez-Canut, V.; Roca, M.; Bertran, J.; Moliner, V.; Tunon, I. *J. Am. Chem. Soc.* **2011**, *133*, 12050.

(40) Barrozo, A.; Duarte, F.; Bauer, P.; Carvalho, A. T.; Kamerlin, S. C. *J. Am. Chem. Soc.* **2015**, *137*, 9061.

(41) Marino, T.; Russo, N.; Toscano, M. *Chemistry* **2013**, *19*, 2185.

(42) Boltes, I.; Czapinska, H.; Kahnert, A.; von Bulow, R.; Dierks, T.; Schmidt, B.; von Figura, K.; Kertesz, M. A.; Uson, I. *Structure* **2001**, *9*, 483.

(43) Bond, C. S.; Clements, P. R.; Ashby, S. J.; Collyer, C. A.; Harrop, S. J.; Hopwood, J. J.; Guss, J. M. *Structure* **1997**, *5*, 277.

(44) Hernandez-Guzman, F. G.; Higashiyama, T.; Pangborn, W.; Osawa, Y.; Ghosh, D. *J. Biol. Chem.* **2003**, *278*, 22989.

(45) Lukatela, G.; Krauss, N.; Theis, K.; Selmer, T.; Gieselmann, V.; von Figura, K.; Saenger, W. *Biochemistry* **1998**, *37*, 3654.

(46) Rivera-Colon, Y.; Schutsky, E. K.; Kita, A. Z.; Garman, S. C. *J. Mol. Biol.* **2012**, *423*, 736.

(47) van Loo, B.; Schober, M.; Valkov, E.; Heberlein, M.; Faber, K.; Hyvonen, M.; Hollfelder, F. *in preparation* **2015**.

(48) Waldow, A.; Schmidt, B.; Dierks, T.; von Bulow, R.; von Figura, K. *J. Biol. Chem.* **1999**, *274*, 12284.

(49) Jonas, S.; van Loo, B.; Hyvonen, M.; Hollfelder, F. *J. Mol. Biol.* **2008**, *384*, 120.

(50) Brandao, T. A.; Hengge, A. C.; Johnson, S. J. *J. Biol. Chem.* **2010**, *285*, 15874.

(51) Hengge, A. C.; Denu, J. M.; Dixon, J. E. *Biochemistry* **1996**, *35*, 7084.

(52) Hengge, A. C.; Edens, W. A.; Elsing, H. *J. Am. Chem. Soc* **1994**, *116*, 5045.

(53) Hengge, A. C.; Sowa, G. A.; Wu, L.; Zhang, Z. Y. *Biochemistry* **1995**, *34*, 13982.

(54) Hengge, A. C.; Zhao, Y.; Wu, L.; Zhang, Z. Y. *Biochemistry* **1997**, *36*, 7928.

(55) Keng, Y. F.; Wu, L.; Zhang, Z. Y. *Eur. J. Biochem.* **1999**, *259*, 809.

(56) McCain, D. F.; Catrina, I. E.; Hengge, A. C.; Zhang, Z. Y. *J. Biol. Chem.* **2002**, *277*, 11190.

(57) McWhirter, C.; Lund, E. A.; Tanifum, E. A.; Feng, G.; Sheikh, Q. I.; Hengge, A. C.; Williams, N. H. *J. Am. Chem. Soc.* **2008**, *130*, 13673.

(58) Zhang, Y. L.; Hollfelder, F.; Gordon, S. J.; Chen, L.; Keng, Y. F.; Wu, L.; Herschlag, D.; Zhang, Z. Y. *Biochemistry* **1999**, *38*, 12111.

(59) Williams, S. J.; Denehy, E.; Krenske, E. H. *J. Org. Chem.* **2014**, *79*, 1995.

(60) O'Brien, P. J.; Herschlag, D. *Chem. Biol.* **1999**, *6*, R91.

(61) Khersonsky, O.; Tawfik, D. S. *Annu. Rev. Biochem.* **2010**, *79*, 471.

(62) Babtie, A. C.; Bandyopadhyay, S.; Olguin, L. F.; Hollfelder, F. *Angew. Chem. Int. Ed. Engl.* **2009**, *48*, 3692.

(63) Mohamed, M. F.; Hollfelder, F. *Biochim. Biophys. Acta* **2013**, *1834*, 417.

(64) Jonas, S.; Hollfelder, F. *Pure Appl. Chem.* **2009**, *81*, 731.

(65) Jensen, R. A. *Annu. Rev. Microbiol.* **1976**, *30*, 409.

(66) O'Brien, P. J.; Herschlag, D. *J. Am. Chem. Soc.* **1998**, *120*, 12369.

(67) Bielicki, J.; Fuller, M.; Guo, X. H.; Morris, C. P.; Hopewood, J. J.; Anson, D. S. *Biochem. J.* **1995**, *311*, 333.

(68) Bielicki, J.; Hopwood, J. J. *Biochem. J.* **1991**, *279*, 515.

(69) Kintses, B.; Hein, C.; Mohamed, M. F.; Fischlechner, M.; Courtois, F.; Laine, C.; Hollfelder, F. *Chem. Biol.* **2012**, *19*, 1001.

(70) Lassila, J. K.; Zalatan, J. G.; Herschlag, D. *Annu. Rev. Biochem.* **2011**, *80*, 669.

(71) Beil, S.; Kehrli, H.; James, P.; Staudenmann, W.; Cook, A. M.; Leisinger, T.; Kertesz, M. A. *Eur. J. Biochem.* **1995**, *229*, 385.

(72) Hummerjohann, J.; Laudenbach, S.; Retey, J.; Leisinger, T.; Kertesz, M. A. *J. Bacteriol.* **2000**, *182*, 2055.

(73) von Bülow, R.; Schmidt, B.; Dierks, T.; von Figura, K.; Uson, I. *J. Mol. Biol.* **2001**, *305*, 269.

(74) Appel, M. J.; Bertozzi, C. R. *ACS Chem. Biol.* **2015**, *10*, 72.

(75) Benkovic, S. J.; Benkovic, P. A. *J. Am. Chem. Soc.* **1966**, *88*, 5504.

(76) Admiraal, S. J.; Herschlag, D. *Chem. Biol.* **1995**, *2*, 729.

(77) Labow, B. I.; Herschlag, D.; Jencks, W. P. *Biochemistry* **1993**, *32*, 8737.

(78) Chapman, E.; Bryan, M. C.; Wong, C. H. *Proc. Natl. Acad. Sci. U. S. A.* **2003**, *100*, 910.

(79) Chapman, E.; Best, M. D.; Hanson, S. R.; Wong, C. H. *Angew. Chem. Int. Ed. Engl.* **2004**, *43*, 3526.

(80) Hopkins, A.; Day, R. A.; Williams, A. *J. Am. Chem. Soc.* **1983**, *105*, 6062.

(81) Benkovic, S. J.; Vergara, E. V.; Hevey, R. C. *J. Biol. Chem.* **1971**, *246*, 4926.

(82) Dodgson, K. S.; Spencer, B.; Williams, K. *Biochem. J.* **1956**, *64*, 216.

(83) Zalatan, J. G.; Fenn, T. D.; Brunger, A. T.; Herschlag, D. *Biochemistry* **2006**, *45*, 9788.

(84) Fendler, E. J.; Fendler, J. H. *J. Org. Chem.* **1968**, *33*, 3852.

(85) Kirby, A. J.; Jencks, W. P. *J. Am. Chem. Soc.* **1965**, *87*, 3209.

(86) Kirby, A. J.; Vargolis, A. G. *J. Am. Chem. Soc.* **1967**, *89*, 415.

(87) Herschlag, D.; Jencks, W. P. *J. Am. Chem. Soc.* **1989**, *111*, 7587.

(88) Anslyn, E. V.; Dougherty, D. A. *Modern Physical Organic Chemistry*; University Science Books: USA, 2006.

(89) Cleland, W. W. In *Isotope Effects in Chemistry and Biology,* ; Kohen, A., Limbach, H.-H., Eds.; CRC Press: Boca Raton, 2006, p 915.

(90) Hengge, A. C. *Acc. Chem. Res.* **2002**, *35*, 105.

(91) Hengge, A. C. *FEBS Lett.* **2001**, *501*, 99.

(92) Hoff, R. H.; Larsen, P.; Hengge, A. C. *J. Am. Chem. Soc.* **2001**, *123*, 9338.

(93) Kuznetsov, V. I.; Hengge, A. C. *Biochemistry* **2013**, *52*, 8012.

(94) Bobyr, E.; Lassila, J. K.; Wiersma-Koch, H. I.; Fenn, T. D.; Lee, J. J.; Nikolic-Hughes, I.; Hodgson, K. O.; Rees, D. C.; Hedman, B.; Herschlag, D. *J. Mol. Biol.* **2012**, *415*, 102.

(95) Sengerova, B.; Tomlinson, C.; Atack, J. M.; Williams, R.; Sayers, J. R.; Williams, N. H.; Grasby, J. A. *Biochemistry* **2010**, *49*, 8085.

(96) Dierks, T.; Miech, C.; Hummerjohann, J.; Schmidt, B.; Kertesz, M. A.; von Figura, K. *J. Biol. Chem.* **1998**, *273*, 25560.

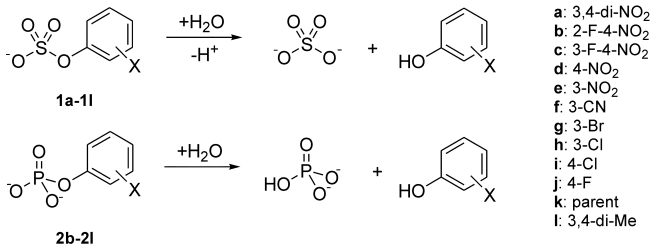

Scheme 1. General reaction scheme for the PAS-catalyzed hydrolysis of aryl sulfate monoesters **1a**-**1l** and aryl phosphate monoesters **2b**-**2l**.

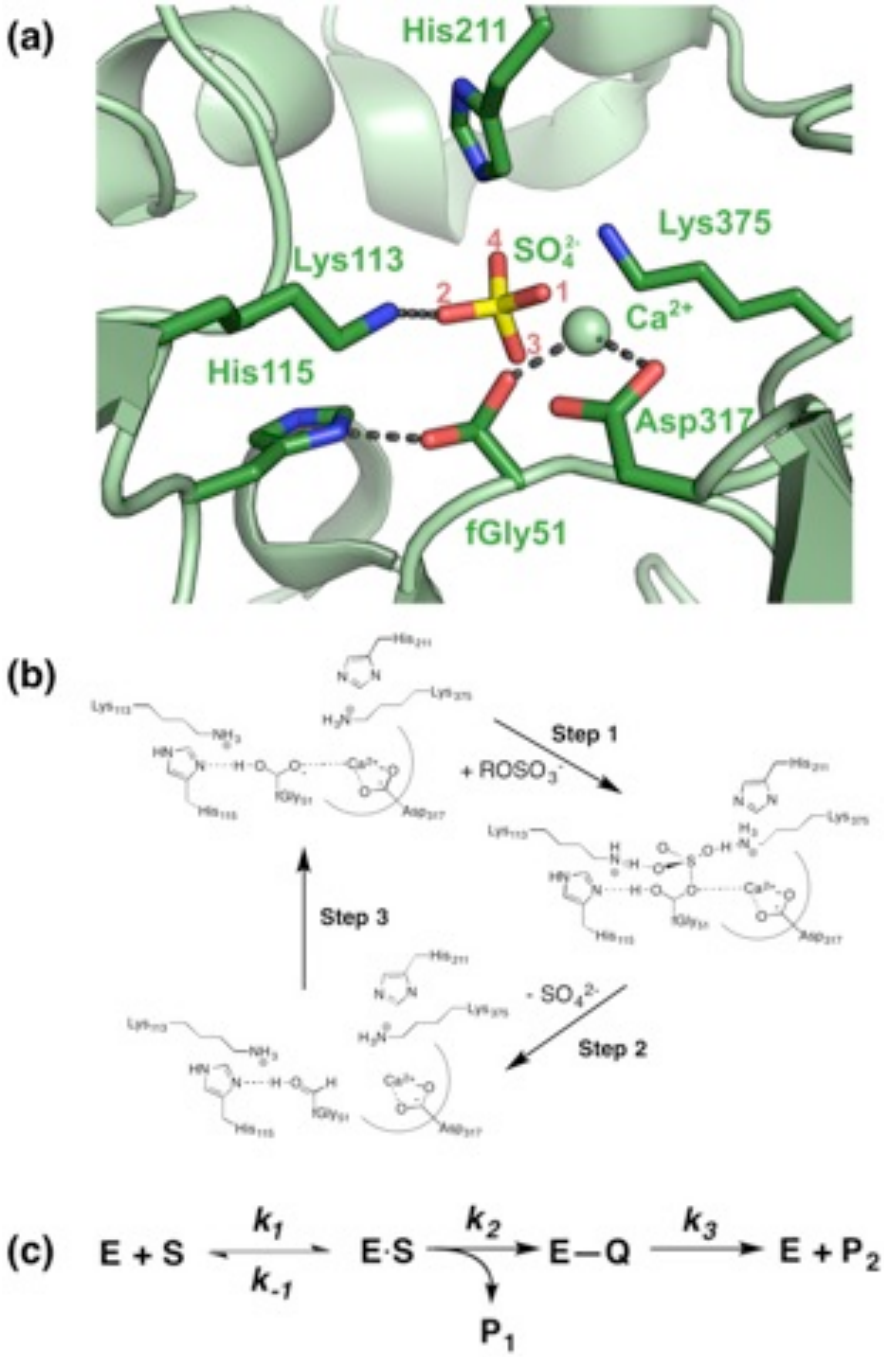

Figure 1. Active site and reaction mechanism of PAS. (**a**) 3D representation of the active site of PAS with a bound sulfate ion.[42]. The assignment of the analogous non-bridging (O_1-O_3) and bridging (O_4) oxygens in the sulfate ester substrate were based on positions of

the active site residues in the X-ray structure of human arylsulfatase A C69A[73] with *p*-nitrocatechol sulfate bound in the active site. (**b**) Proposed catalytic pathway for PAS-catalyzed sulfate monoester hydrolysis. Upon binding of the sulfate monoester substrate, the hydrated fGly51 performs a nucleophilic attack on the sulfur atom and the bond to the alcohol leaving group (ROH) is broken (S-O_{bridge} bond fission) (Step 1). The covalent intermediate is broken down by base-catalyzed hemiacetal cleavage in which inorganic sulfate acts as the leaving group (Step 2). The enzyme is subsequently regenerated by hydration of the formylglycine aldehyde (step 3). (**c**) Schematic representation of the steps in panel **b**. k_1 is the rate of formation of the enzyme-substrate (E·S) complex from free enzyme (E) and substrate (S) and k_{-1} represents the dissociation rate of the ES-complex. k_2 is the rate constant for the nucleophilic attack of the hydrated formylglycine and subsequent S-O_{bridge} bond fission (step 1), and k_3 that of hemiacetal cleavage (step 2). The rehydration of the fGly residue (step 3) is expected to be several orders faster that hemiacetal cleavage, and thus was not considered for the interpretation of pre-steady state kinetics. Product P_1 is the phenolate leaving group expelled from the substrate in step 1; product P_2 is inorganic sulfate.

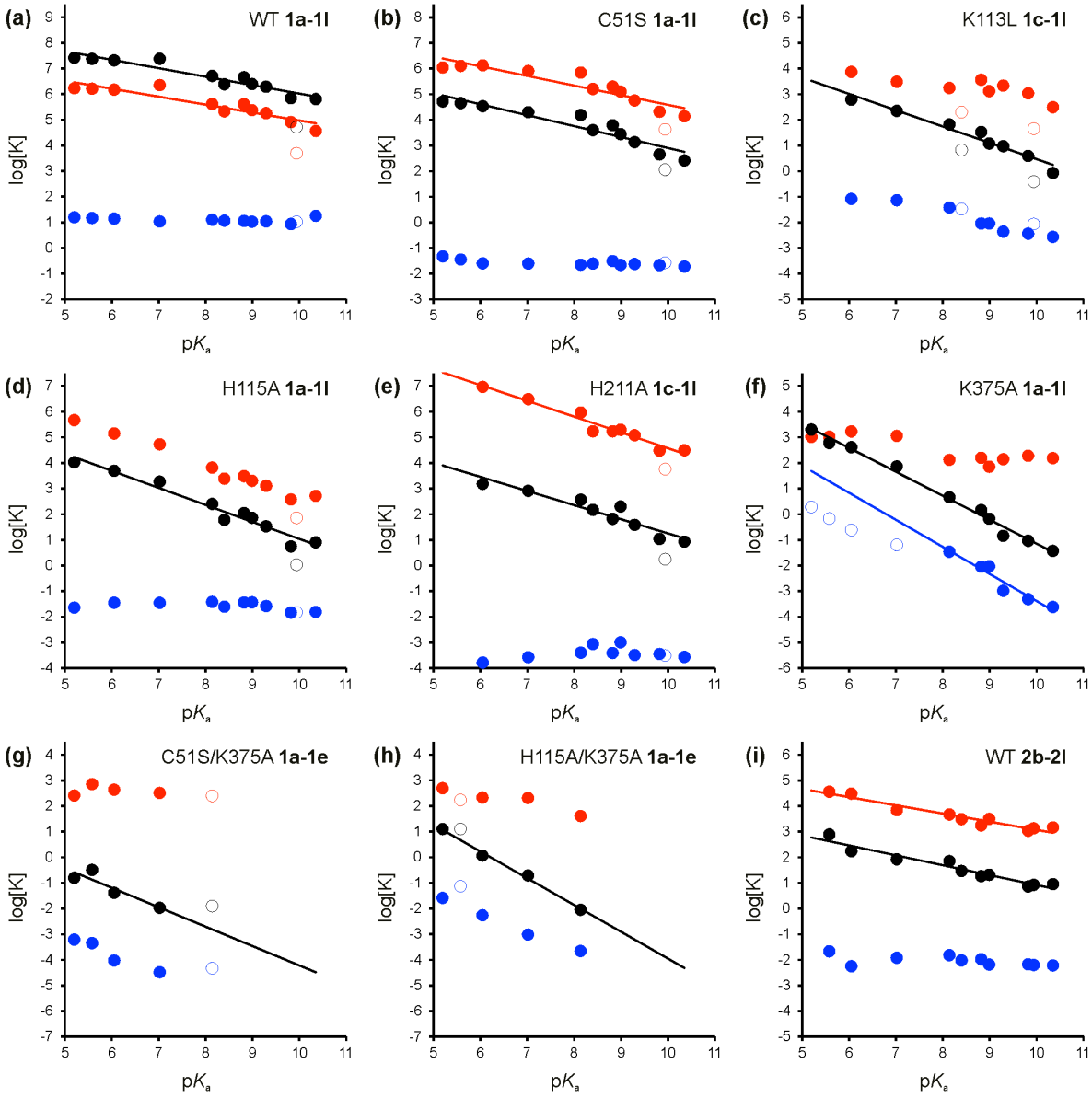

Figure 2. Dependence of catalytic parameters k_{cat} (blue) $1/K_M$ (red) and k_{cat}/K_M (black) (log-values) for PAS-catalyzed hydrolysis of sulfate monoesters on leaving group ability (as represented by the pK_a of the free phenol in solution). (**a**) PAS WT; (**b**) PAS C51S; (**c**) PAS K113L; (**d**) PAS H115A; (**e**) PAS H211A; (**f**) PAS K375A; (**g**) PAS C51S/K375A; (**h**) PAS H115A/K375A. (**i**) PAS WT with phosphate monoesters. All data were obtained in 100 mM Tris-HCl pH 8.0; 500 mM NaCl at 25 ˚C. The resulting slopes ($=\beta_{leaving\ group}^{obs}$) are listed in Table 1 and S14. The data for sulfate monoester **1k** deviated significantly from the trend for

all enzymes, suggesting a consistent difference in binding constant as compared to the other sulfate monoester substrates and were therefore not included in any of the fits. Data points represented by open circles were not included in the fits. All data for the kinetic parameters are listed in the supporting information (Table S1, S3-S10).

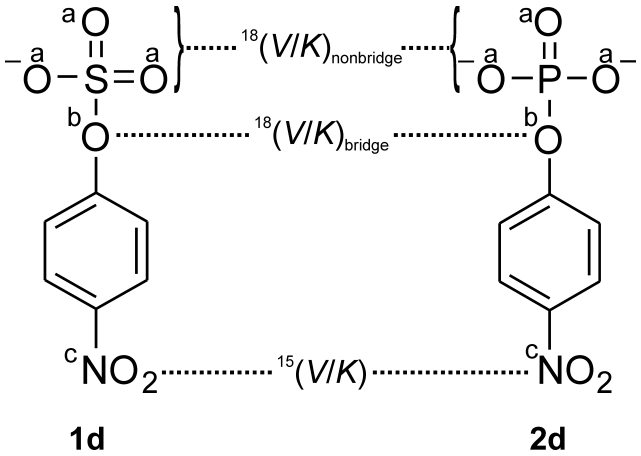

Figure 3. Positions for the kinetic isotope effect measurements in sulfate monoester **1d** and phosphate monoester **2d.** Effects were measured for the nonbridging oxygens (a, $^{18}O_{nonbridge}$ KIE), bridging oxygen (b, $^{18}O_{bridge}$ KIE), and for the nitro group (c, ^{15}N KIE). See Chart S1 (SI) for the structures of the labeled compounds used.

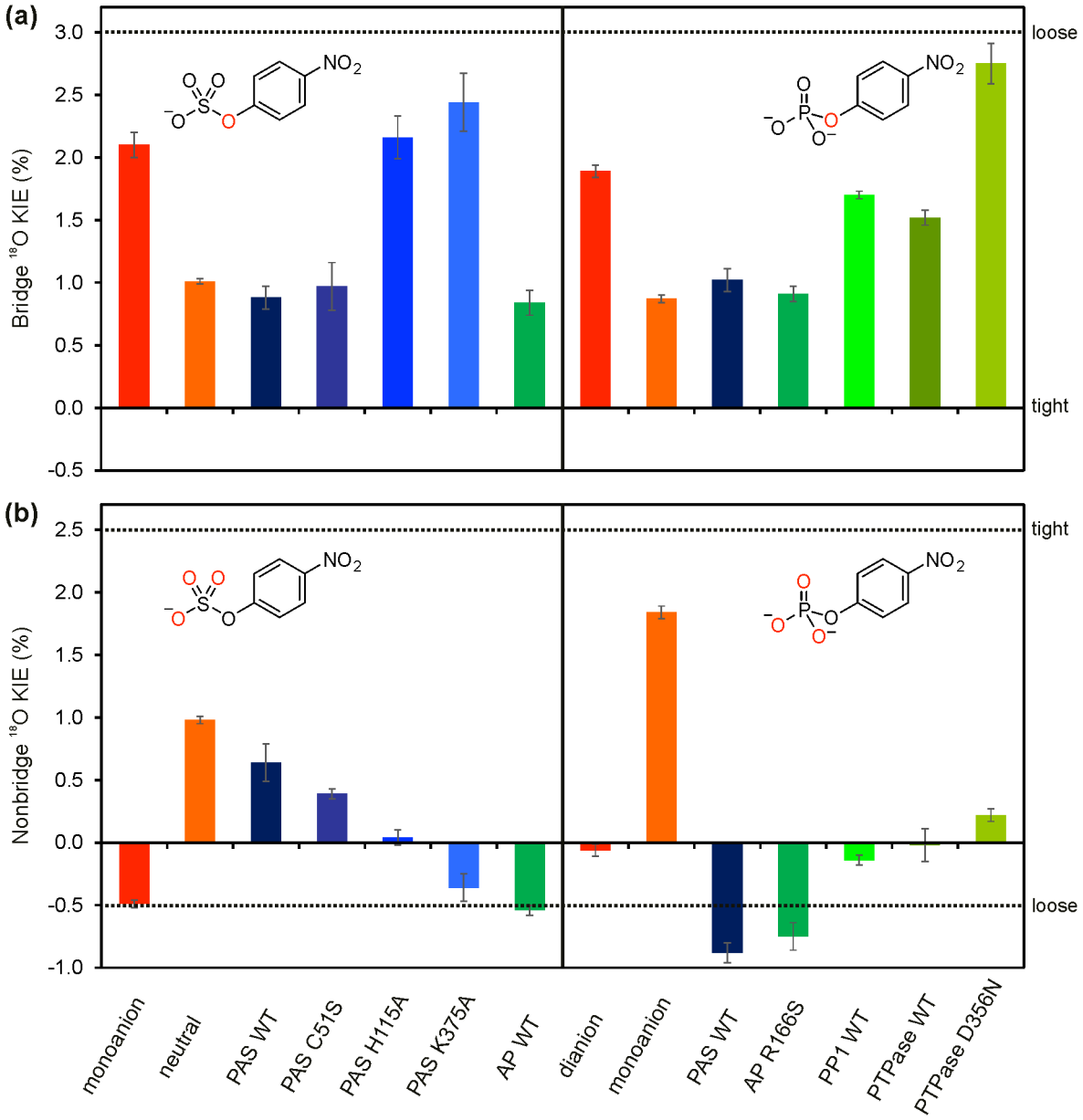

Figure 4. Kinetic Isotope Effects (KIEs) for PAS-catalyzed hydrolysis of sulfate monoester **1d** and phosphate monoester **2d**. The values are listed in Table 3 (PAS and solution data) and Table S15 (all other enzymatic data, SI). (**a**) The ^{18}O-KIEs for the bridging (or leaving group) oxygen. (**b**) The ^{18}O-KIEs for the nonbridging oxygens. The dotted lines indicate extremes of ^{18}O KIEs for tight (^{18}O bridge = 0%, ^{18}O non-bridge = +2.5%) and loose (^{18}O bridge = +3.0%, ^{18}O non-bridge = -0.5%) transition states.[90] AP: *E. coli* Alkaline

phosphatase,[20] PP1: Protein Phosphatase 1,[57] PTPase: *Yersinia* Protein Tyrosine Phosphatase.[53]

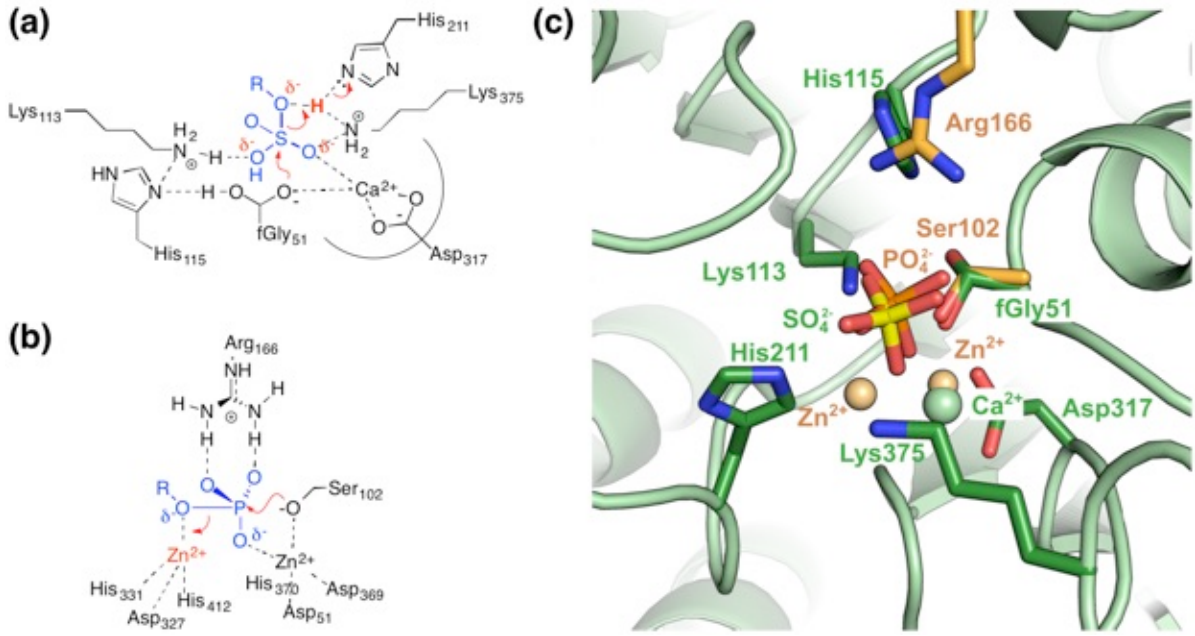

Figure 5. Comparison of mechanisms of leaving group stabilization in the transition states of sulfate monoester hydrolysis by PAS and phosphate monoester hydrolysis by alkaline phosphatase. (**a**) During fission of the sulfate ester bond negative charge develops on the leaving group and is offset by a proton, held by the H211-K375 pair. (**b**) In *E. coli* alkaline phosphatase (AP)[25,28] the charge developing on the leaving group as a serine nucleophile attacks is offset by a metal ion. (**c**) Structural superposition of PAS[42] (pdb entry 1HDH) and AP[94] (3TG0), including bound product in the active site (inorganic sulfate and phosphate, respectively. The functionally homologous residues align well, showing that the second divalent metal ion (Zn^{2+}) of AP is providing charge offset in a similar position as the proton held by H211 and K375 in PAS.

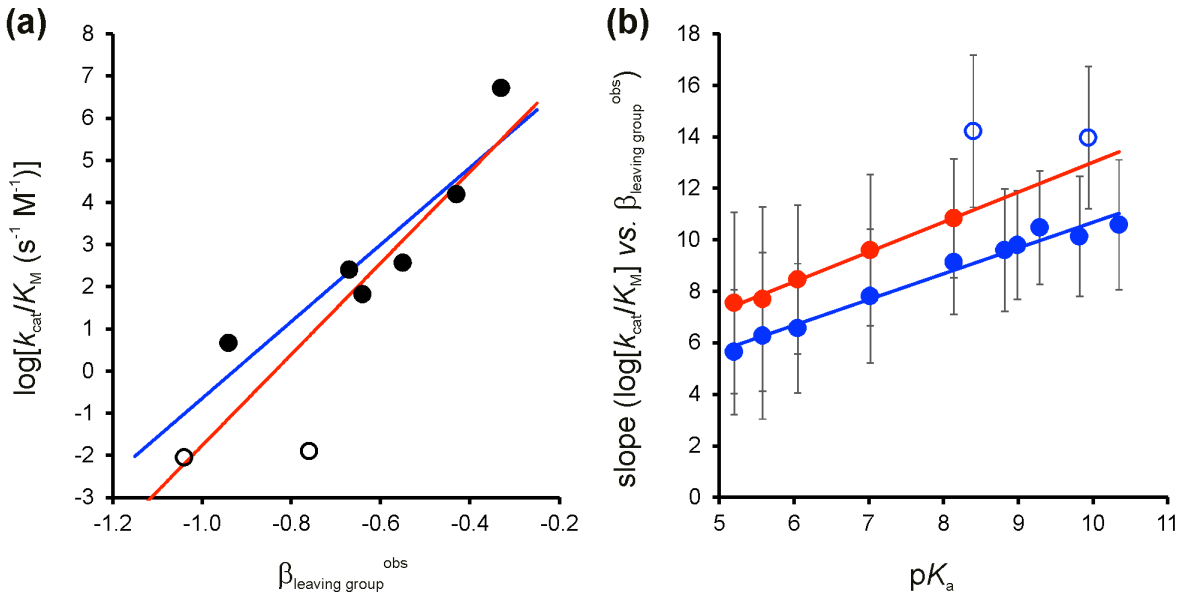

Figure 6. PAS variants with lower catalytic efficiencies are more sensitive to the leaving group ability. (**a**) Correlation between catalytic efficiency (represented by $\log[k_{cat}/K_M]$) and leaving group dependency ($\beta_{leaving\ group}^{obs}$) of the various PAS variants (closed symbols: PAS WT and its single mutants, open symbols: double mutants) for 3-nitrophenyl sulfate **1e**. Linear correlations including all variants (red line, $R^2 = 0.79$; $p = 0.0033$) and only including the single mutants and wild type (blue line, $R^2 = 0.83$; $p = 0.011$) show slopes of 10.8±2.3 and 9.1±2.0 respectively. (**b**) Correlation between the response slope as shown in panel (**a**) and pK_a values of the substrate's leaving group (see Figure S14 for the corresponding correlation lines). The slopes for sulfate monoesters **1f** and **1k** clearly deviate from the observed trend and were therefore not included in the fit (for more details see Figure S15, SI). Red fit: slope: 1.16±0.05; R^2: 0.99; p: 2.2×10^{-4}. Blue fit: slope: 1.0±0.06; R^2: 0.97; p: $<10^{-4}$.

Table 1. Overview of the observed Brønsted constants for leaving group dependence ($\beta_{leaving\ group}^{obs}$) of k_{cat}/K_M for PAS-catalyzed sulfate and phosphate monoester hydrolysis.[a]

Reaction	catalyst	$\beta_{leaving\ group}^{obs}$
Sulfate monoesters	Solution (neutral)	-0.27[b]
	Solution (monoanion)	-1.81[b]
	WT	-0.33±0.04
	C51S	-0.43±0.05
	K113L	-0.64±0.06
	H115A	-0.67±0.05
	H211A	-0.55±0.07
	K375A	-0.94±0.04
	C51S/K375A	-0.76±0.24
	K113L/K375A	nd[c]
	H115A/K375A	-1.04±0.06
	H211A/K375A	nd[c]
Phosphate monoesters	Solution (monoanion)	-0.27[d]
	Solution (dianion)	-1.23[d]
	WT	-0.39±0.04

[a]All enzymatic reactions performed in 100 mM Tris-HCl pH 8.0, 500 mM NaCl, 25 °C. [b]Edwards *et al.*[3], H_2O as the nucleophile. [c]Not determined. Activity too low to be detectable. [d]Kirby & Vargolis[86], H_2O as the nucleophile.

Table 2. Effect of mutations on leaving group dependence for PAS-catalyzed sulfate monoester hydrolysis in PAS WT and K375A

mutation	reaction	effect in	$\Delta\beta_{leaving\ group}^{obs}$
C51S	**1a-1l**	WT	+0.10±0.04[a]
	1a-1d	K375A	+0.01±0.33[b]
K113L	**1c-1l**	WT	+0.24±0.05[a]
H115A	**1a, 1c-1l**	WT	+0.32±0.03[a]
	1a-1l	K375A	+0.15±0.05[b]
H211A	**1c-1l**	WT	+0.16±0.07[a]
K375A	**1a-1e**	WT	+0.61±0.03[a]

[a]Determined as the slope for $\log[(k_{cat}/K_M)_{WT}/(k_{cat}/K_M)_{mutant}]$ plotted *vs*. leaving group pK_a (Figure S10a). [b]Determined as the slope for $\log[(k_{cat}/K_M)_{K375A}/(k_{cat}/K_M)_{double\ mutant}]$ plotted *vs*. leaving group pK_a (Figure S10b, SI).

Table 3. Kinetic isotope effects for PAS-catalyzed hydrolysis of sulfate monoester **1d** and phosphate monoester **2d**.

substrate	catalyst	$^{15}(V/K)$	$^{18}(V/K)_{bridge}$	$^{18}(V/K)_{nonbridge}$
1d	solution (neutral)[a]	1.0004 (1)	1.0101 (2)	1.0098 (3)
	solution (monoanion)[b]	1.0026 (1)	1.0210 (10)	0.9951 (3)
	WT	1.0006 (4)	1.0088 (9)	1.0064 (15)
	C51S	1.0012 (6)	1.0097 (19)	1.0039 (4)
	H115A	1.0013 (2)	1.0216 (17)	1.0004 (6)
	H211A[c]	-	-	-
	K375A	1.0023 (5)	1.0244 (23)	0.9958 (11)
2d	solution (monoanion)[d]	1.0004 (2)	1.0087 (3)	1.0184 (5)
	solution (dianion)[d]	1.0028 (2)	1.0189 (5)	0.9994 (5)
	WT	1.0007 (4)	1.0102 (9)	0.9912 (8)

[a]Recorded in 10 N HCl, 15 °C.[92] [b]Recorded at pH 9.0, 85 °C.[92] [c]Activity too low to be determined. [d]Recorded at 95 °C.[52]